Induction of ferroptosis and apoptosis in endometrial cancer cells by dihydroisotanshinone I

Ching-Yuan Wu [a,b,c,*], Yao-Hsu Yang [a,b], Yu-Shih Lin [d], Li-Hsin Shu [a], Hung-Te Liu [a], Yu-Huei Wu [e], Yu-Heng Wu [f]

[a] Department of Chinese Medicine, Chiayi Chang Gung Memorial Hospital, Chiayi, Taiwan
[b] School of Chinese Medicine, College of Medicine, Chang Gung University, Tao-Yuan, Taiwan
[c] Research Center for Chinese Herbal Medicine, College of Human Ecology, Chang Gung University of Science and Technology, Taoyuan, Taiwan
[d] Department of Pharmacy, Chiayi Chang Gung Memorial Hospital, Chiayi, Taiwan
[e] Department of Biomedical Sciences, Chang Gung University, Tao-Yuan, Taiwan
[f] Department of Electrical Engineering, National Sun Yat-Sen University, Kaohsiung, Taiwan

ABSTRACT

Danshen, also known as *Salvia miltiorrhiza*, is a medicinal herb used in traditional Chinese medicine. Its potential impact on endometrial cancer has not been thoroughly investigated. This study aimed to examine the effect of dihydroisotanshinone I (DT), a compound found in Danshen, on the viability of ARK1 and ARK2 endometrial cancer cells and its mechanisms. The results showed that 10 μM DT inhibited cell viability of ARK1 and ARK2 cells by inducing apoptosis and ferroptosis, which was achieved by blocking the expression of GPX4. In vivo experiments using a xenograft nude mouse model indicated that DT treatment significantly reduced tumor volume without causing any adverse effects. These findings suggest that DT may be a potential therapeutic agent for inhibiting endometrial cancer cell viability, but further research is needed to confirm these results.

1. Introduction

Endometrial cancer is a common gynecological malignancy in the US and other countries. While the prognosis for early-stage endometrial cancer is generally positive, around one-third of patients receive a diagnosis at an advanced stage [1]. The 5-year overall survival rate for stage IV endometrial cancer is reported to be between 0 and 18 % [2,3]. Treatment methods for endometrial cancer encompass surgery, chemotherapy, and radiotherapy. In situations where metastatic or recurrent disease cannot be cured, anti-estrogenic medications may serve as alternative therapies [4]. However, the efficacy of these treatments is limited, as widely metastatic recurrences of endometrial cancer are often fatal, and none of the treatments are curative [4].

Ferroptosis, a regulated cell death process, depends on iron and reactive oxygen species (ROS) and is characterized by lipid peroxidation [5]. A phospholipid hydroperoxidase called glutathione (GSH) peroxidase 4 (GPX4) is essential for preventing the formation of toxic lipid ROS, which depend on iron (Fe2+) [6]. When GPX4 function is inhibited, lipid-based ROS, particularly lipid hydroperoxides, accumulate and ultimately induce ferroptosis [7,8]. Ferroptosis, unlike apoptosis, is a non-apoptotic process. Increasing evidence suggests that ferroptosis plays a key role in controlling the growth of various cancer cells [9]. Moreover, a previous study

A
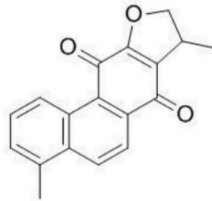
Dihydroisotanshinone I

B   **ARK1 cells**
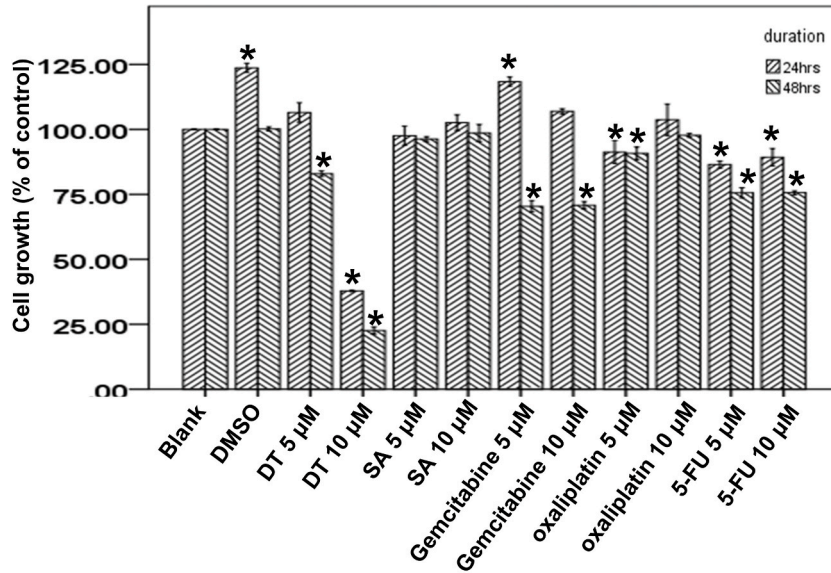
C   **ARK2 cells**
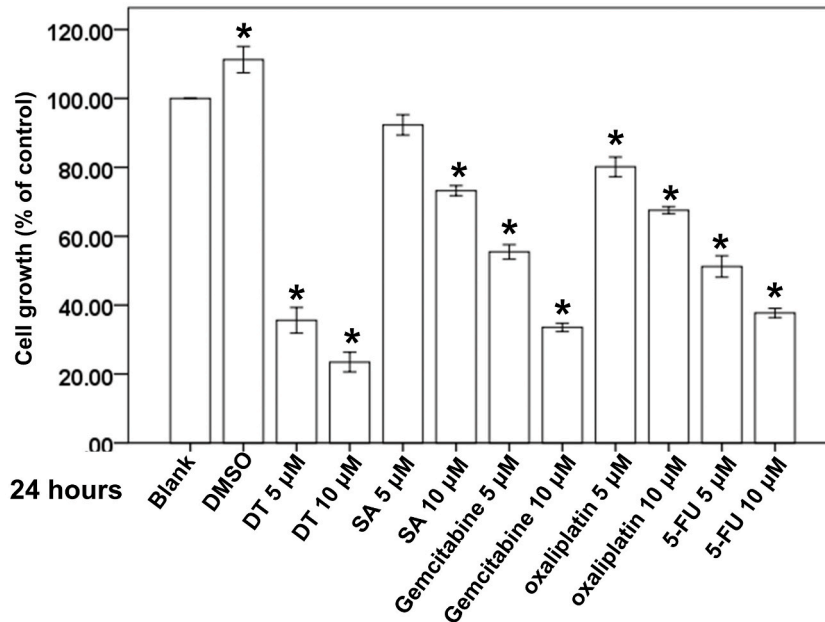
(caption on next page)

Fig. 1. The effect of DT on cell viability of endometrial cancer cell lines. **A** The structure of dihydroisotanshinone I (DT). **B, C** ARK1 cells (B) or ARK2 cells (C) were measured by XTT assay after indicated hours of culturing in the presence of indicated compounds. All the results are representative of at least three independent experiments. (Error bars = mean ± S.E.M. Asterisks (*) mark samples significantly different from DMSO group with $p < 0.01$.).

showed that early-stage endometrial cancer had higher levels of GPX4 and glutathione synthetase (GSS) than normal tissues, as identified through proteomic analysis, suggesting that GPX4-suppressed ferroptosis may be critical in endometrial cancer development [9,10]. Targeting ferroptosis has also shown potential for effectively overcoming drug resistance in endometrial cancer.

This study found that dihydroisotanshinone I (DT) (Fig. 1A), derived from the dried roots of *Salvia miltiorrhiza Bunge*, had inhibitory effects on the viability of endometrial cancer cell lines (ARK1 and ARK2 cells). DT was observed to inhibit GPX4 expression and induce ferroptosis by causing lipid peroxidation. In addition, DT treatment (30 mg/kg via intraperitoneal injection) significantly reduced tumor growth without adverse effects in a nude mouse model. These results indicate that DT could be a promising therapeutic strategy for treating endometrial cancer.

2. Methods and materials

2.1. Cell culture and treatment

ARK1 cells and ARK2 cells, which are cell lines derived from human endometrial serous adenocarcinoma, were kindly gifts from Dr. Tzu-Hao Wang (Department of Obstetrics and Gynecology, Chang Gung Memorial Hospital and Chang Gung University) and cultured in RPMI-1640 medium supplemented with 10 % fetal bovine serum at 37 °C and 5 % CO2. Dihydroisotanshinone I, a compound with a purity of 98 % and solubility of >5 mg/mL in DMSO, was obtained from ChemFaces Natural Products Co., Ltd., China (Catalog number: CFN-90162; PubChem CID:89406). The cells were cultured to 60–70 % confluence before being treated with the indicated compounds in DMSO at the specified concentrations. Control cells were treated with DMSO alone.

2.2. XTT (2,3-Bis-(2-Methoxy-4-Nitro-5-Sulfophenyl)-2H-Tetrazolium-5-Carboxanilide) assay

The cells were seeded in 96-well plates at a density of 1×10^3 cells per well in a medium supplemented with 10 % FBS. After allowing the cells to attach, the old medium was replaced with fresh medium containing 10 % FBS, and the cells were treated with the designated drugs for a specified time. The XTT assay kit (Biological Industries, ISRAEL, catalog number: 20-300-1000) was used to measure the absorbance, in accordance with the manufacturer's instructions. The XTT formazan complex was quantitatively measured at 492 nm using an ELISA reader (Bio-Rad Laboratories, Inc., Hercules, CA, USA).

2.3. Flow cytometry for apoptosis

The procedure used to analyze apoptosis via flow cytometry was carried out in the same manner as described previously [11]. First, the cells were seeded at a density of 1×10^6 cells in a 100-mm plate and allowed to culture overnight before being treated with the specified compounds for a predetermined period. Subsequently, the treated cells were collected by centrifugation, and the medium was discarded. To detect apoptosis, the cells were resuspended and subjected to either the Annexin V-FITC Apoptosis Detection Kit (Strong Biotech Corporation, Taiwan, catalog number: AVK250) or the Mitoscreen JC-1 kit (Becton, Dickinson and Company, Franklin Lakes, NJ, USA, catalog number: 551302), according to the manufacturer's instructions. The apoptosis of cells at different developmental stages was analyzed using the BD FACSCanto flow cytometer (Becton, Dickinson and Company, Franklin Lakes, NJ, USA) by gating the corresponding population in the Dot Plots.

2.4. Western blot analysis

The cellular extracts obtained after the specified treatments were collected and prepared using the previously described method for Western blot analysis [12]. Equal amounts of protein were separated by fractionation on a 10 % SDS-PAGE and transferred to polyvinylidene difluoride membranes. The membranes were blocked with 5 % nonfat dried milk for 30 min. Next, the membranes were incubated with the indicated primary antibody for 12 h at room temperature. The list of these primary antibodies were: anti-STAT3 antibody (Cell Signaling, ratio: 1:1000), anti-p-STAT3 antibody (the phosphorylation of STAT3 at Tyr705, Cell Signaling, ratio: 1:1000), anti-SKP2 antibody (Cell Signaling, ratio: 1:1000), anti-PARP antibody (Cell Signaling, ratio: 1:1000), anti-GPX4 antibody (proteintech, ratio: 1:1000) anti-β-actin antibody (Santa Cruz, IB: 1:10000) and anti-GAPDH antibody (Santa Cruz, IB: 1:10000). The primary antibodies and secondary antibodies were diluted in 0.1 % TBST (Tris-Buffered Saline Tween-20) with 1 % nonfat dried milk. The membranes were washed with 0.1 % TBST and then incubated with horseradish peroxidase-conjugated anti-mouse or anti-rabbit secondary antibodies (ratio: 1:5000, Santa Cruz) for 1 h at room temperature. The protein signal was detected using the Super Signal substrate (Pierce Biotechology Inc., Rockfort, IL, USA, catalog number: 34087) via chemiluminescence.

A

B

C ARK1 cells
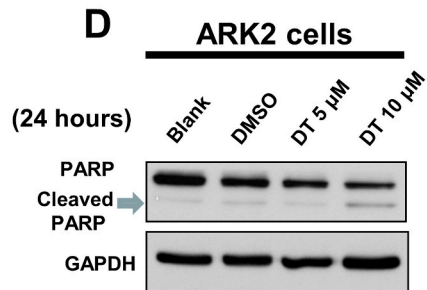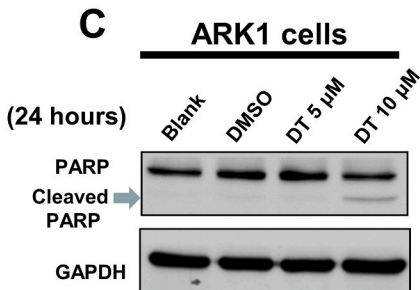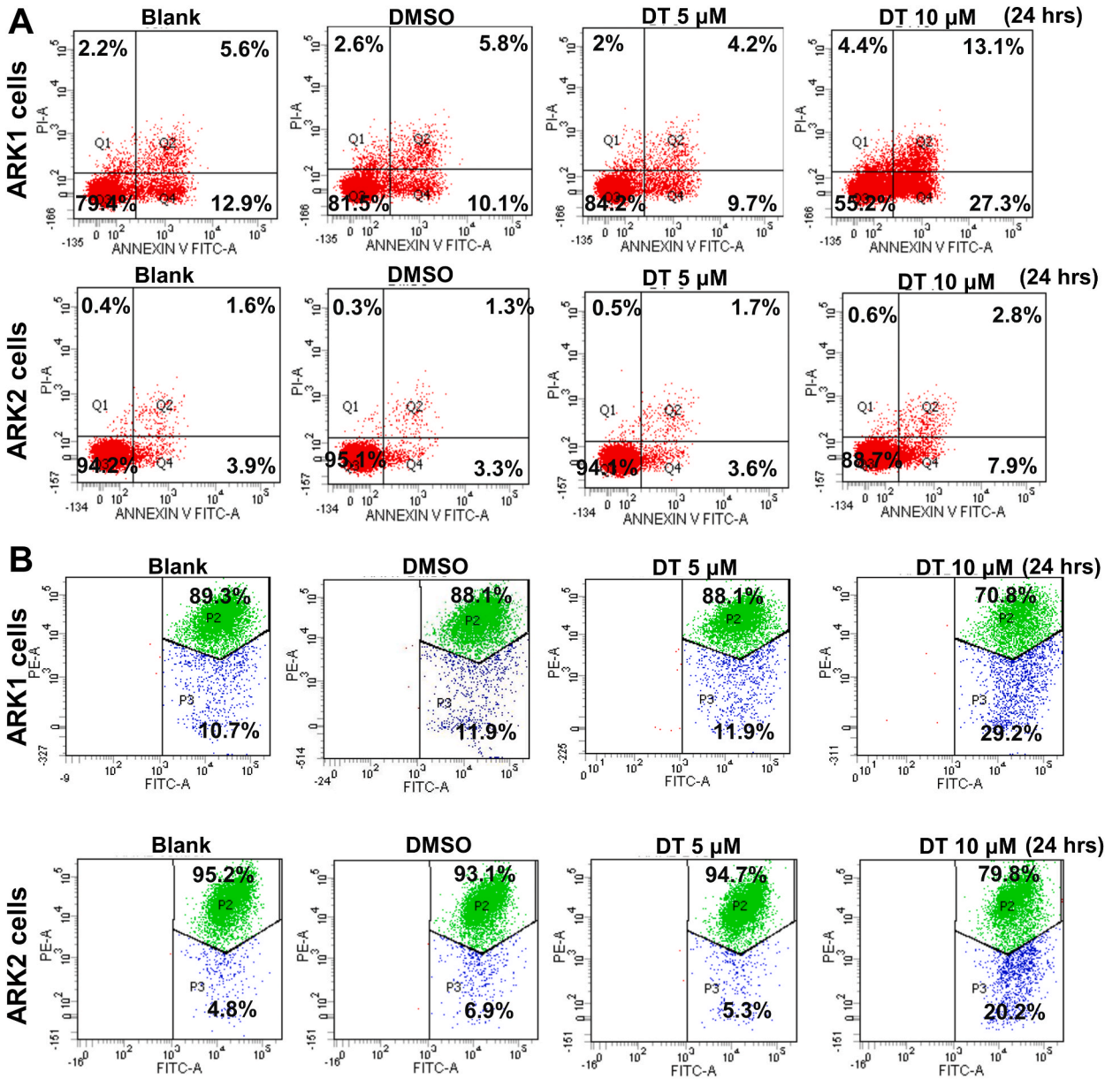
D ARK2 cells

(caption on next page)

Fig. 2. The effect of DT on apoptosis in endometrial cancer cell lines. ARK1 cells or ARK2 cells were treated without or with indicated compounds for 24 h. Cell apoptosis was detected by flow cytometry with annexin-V-FITC/PI dual staining (A) or mitoscreen JC-1 staining (B). **A** For annexin-V-FITC/PI dual staining, the representative histograms of flow cytometric analysis using double staining with annexin-V-FITC (FITC-A) and PI (PI-A). **B** Cell apoptosis was detected by flow cytometry with mitoscreen JC-1 staining. **C, D** Total cell extracts of ARK1 cells (C) or ARK2 cells (D) were harvested from cells treated with DMSO or indicated concentrations of DT for indicated hours. The protein was immunoblotted with polyclonal antibodies specific for PARP. GAPDH was used as an internal loading control. (Error bars = mean ± S.E.M. Asterisks (*) mark samples significantly different from DMSO group with $p < 0.01$.).

2.5. Determination of GSH (reduced Glutathione)/GSSG (oxidized glutathione)

The level of GSH and the ratio of GSH/GSSG in cell extracts was analyzed using the method described previously [13]. Cellular extracts from the indicated cells treated with either DMSO or drugs at indicated concentrations for 24 h were collected and prepared following the manufacturer's instructions. The level of GSH (reduced glutathione)/GSSG (oxidized glutathione) was detected using the Glutathione assay kit (Bioversion, catalog number: K264-100).

2.6. Glutathione peroxidase activity assay

The activity of Glutathione peroxidase (GPX) in cell extracts was analyzed using the method described previously [14]. Cellular extracts of the indicated cells, treated with either DMSO or the designated drug concentrations for 24 h, were collected and prepared in accordance with the manufacturer's instructions. The activity of GPX was determined by measuring the absorption change at 340 nm resulting from NADPH consumption in the presence of H_2O_2, using the Glutathione Peroxidase Activity Colorimetric Assay Kit (Bioversion, catalog number: K762-100). The resulting values were normalized based on cell count.

2.7. Mouse xenograft model

The Animal Care and Use Committee at Chang Gung Memory Hospital approved all protocols utilizing the mouse xenograft model (Approval number: 2020032305). Surgery was conducted under the influence of sodium pentobarbital anesthesia. To establish the xenograft model, 10 male BALB/c-nu female nude mice weighing 18–20g and aged between 5 and 7 weeks were acquired from BioLASCO Taiwan Co., Ltd. Subcutaneous injection of ARK1 cells or ARK2 cells (1×10^6/mouse) was performed in both flanks of the nude mice. After approximately one week, mice with tumor sizes of approximately 10 mm^3 were chosen. The mice were then randomized into two groups with five mice in each group. One group was administered vehicle (2.5 % DMSO) intraperitoneally, while the other group received 30 mg/kg DT every 2 days. Tumor volume and mouse weight were measured every 2–3 days over a period of 3 weeks. Tumor sizes and volume were calculated using the formula: length x width x height x 0.52. The mice were closely monitored daily for tumor size, body weight, and mortality. After two weeks, the mice were euthanized.

2.8. Statistical analyses

The results are presented as mean ± standard error of the mean for the number of replicate samples (n = 3–6, depending on the experiment), and the experiments were repeated at least three times. To evaluate the statistical differences between two groups, an unpaired two-tailed Student's t-test was used. For analysis of more than two groups, ANOVA was conducted, and pairwise group comparisons were assessed using Tukey's test as a post-hoc test in one-way ANOVA. A *p*-value less than 0.01 was considered statistically significant for all comparisons. The calculations were carried out using SPSS version 13.0 (SPSS Inc., Chicago, IL, USA).

3. Results

3.1. The effect of DT on cell viability of endometrial cancer cell lines

In order to investigate the effect of DT obtained from ChemFaces Natural Products Co., Ltd., China (Catalog number: CFN-90162), which has a purity of 98 % for dihydroisotanshinone I and is soluble in DMSO at a concentration of >5 mg/mL, on the growth of endometrial cancer cells, we utilized ARK1 and ARK2 cells as our experimental model and assessed the impact of DT and other compounds using XTT. As previous studies have demonstrated a stronger suppression effect on cell viability of various cancers (including lung and breast cancer) at concentrations of 10 μM or higher for DT [15,16], we selected the concentrations of 5 μM and 10 μM for further investigation. The treatment of ARK1 and ARK2 cells with the indicated compounds for a given duration showed a dose-dependent and time-dependent inhibition of cell viability by DT at concentrations of 5–10 μM (Fig. 1B and C). DT exhibited an IC50 of 9.353 μM and 2.495 μM after being incubated for 24 h on ARK1 and ARK2 cells, respectively. In comparison to SA at 5–10 μM, DT demonstrated a more significant inhibitory effect on cell viability of both ARK1 and ARK2 cells. Notably, at a concentration of 10 μM, DT exhibited a more potent inhibitory effect compared to commonly used clinical anti-cancer agents such as oxaliplatin, gemcitabine, and 5-fluorouracil. Additionally, DT showed the most robust inhibition of cell viability of ARK2 cells, even at a concentration as low as 5 μM. These findings highlight the potential of DT in the suppression of cell viability of human endometrial cancer cells.
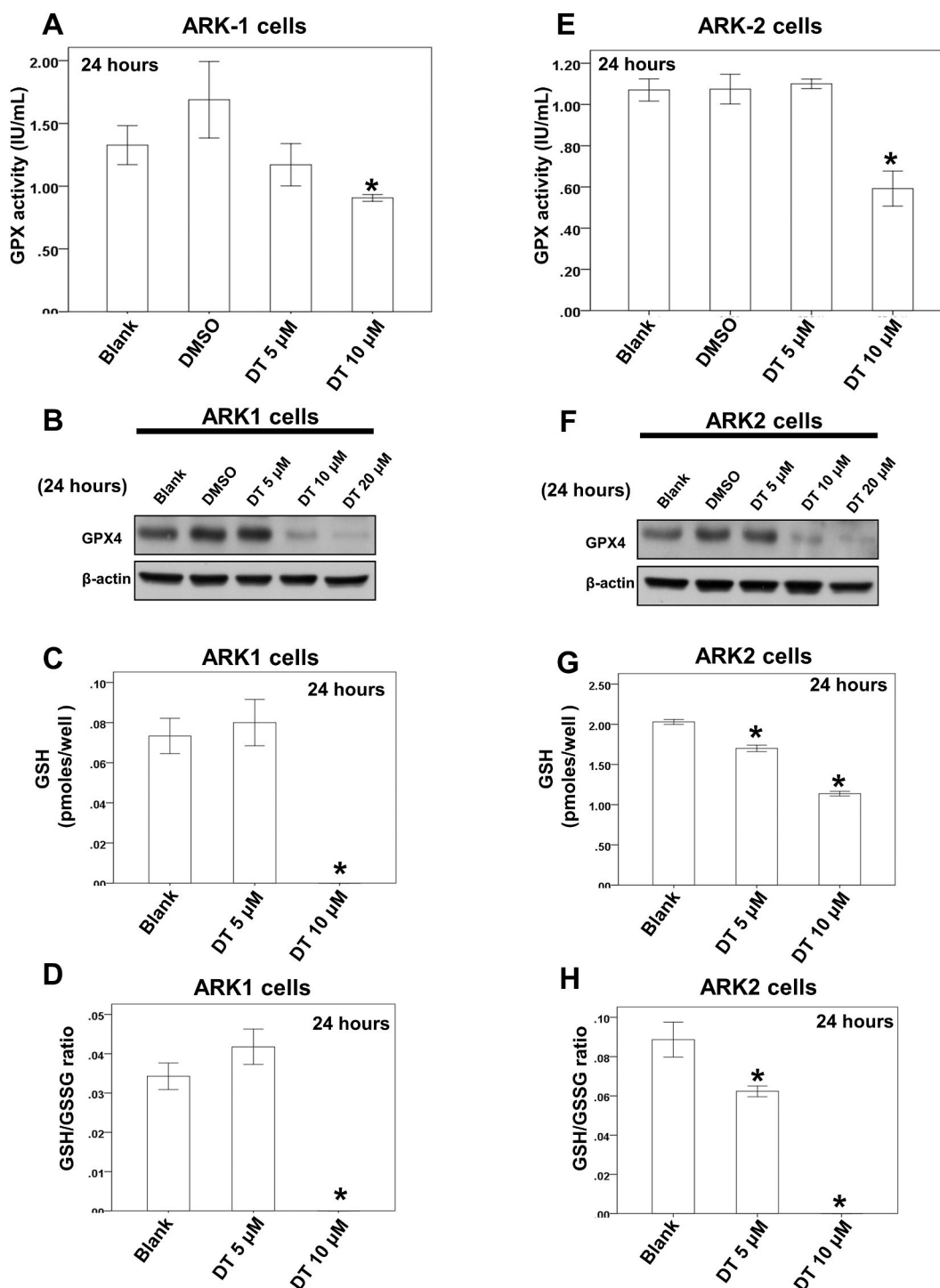
Fig. 3. The effect of DT on ferroptosis of endometrial cancer cells in vitro. **A, E** For GPX activity, ARK1 cells (A) or ARK2 cells (E) were treated with DMSO or indicated drugs for 24 h. Total cell extract was collected and analyzed by GPX activity assay kit. **B, F** Total cell extracts of ARK1 cells (B) or ARK2 cells (F) were harvested from cells treated with DMSO or indicated concentrations of DT for 24 h. The protein was immunoblotted with polyclonal antibodies specific for GPX4. GAPDH was used as an internal loading control. **C, D, G, H** For GSH level and GSH/GSSG ratio, ARK1 cells (C, D) or ARK2 cells (G, H) were treated with DMSO or indicated drugs for 24 h. Total cell extract was collected and analyzed by the Glutathione assay kit. (Error bars = mean ± S.E.M. Asterisks (*) mark samples significantly different from DMSO group with $p < 0.01$.).

3.2. Effects of DT on apoptosis of endometrial cancer cells in vitro

Our prior research has demonstrated that the suppression of certain cancer cell proliferation by DT is linked to apoptosis [12,17]. To investigate the impact of apoptosis on DT treatment for endometrial cancer cells, we conducted an experiment where ARK1 cells and ARK2 cells were treated with indicated compounds for 24 h. Apoptosis was then analyzed using flow cytometry with Annexin V/PI dual staining. The findings revealed that the ARK1 cells and ARK2 cells showed dose-dependent apoptosis after 24 h of treatment with 10 μM DT (Fig. 2A). Additionally, the JC-1 staining assay showed that 10 μM DT resulted in mitochondrial depolarization of ARK1 cells and ARK2 cells in a dose-dependent manner after 24 h (Fig. 2B). As the significant apoptosis effect was observed in ARK1 cells and ARK2 cells when treated with 10 μM DT, we further found that this concentration of DT could upregulate the expression of cleaved PARP, a critical apoptotic protein, in both cell lines (Fig. 2C and D). These findings imply that DT induces apoptosis as a mode of cell death in endometrial cancer cells.

3.3. Induction of ferroptosis by DT in endometrial cancer cells through downregulation of GPX4 expression

The GSH system, composed of GSH and GSSG, is the main pathway that limits ferroptosis [18]. This system plays a crucial role in
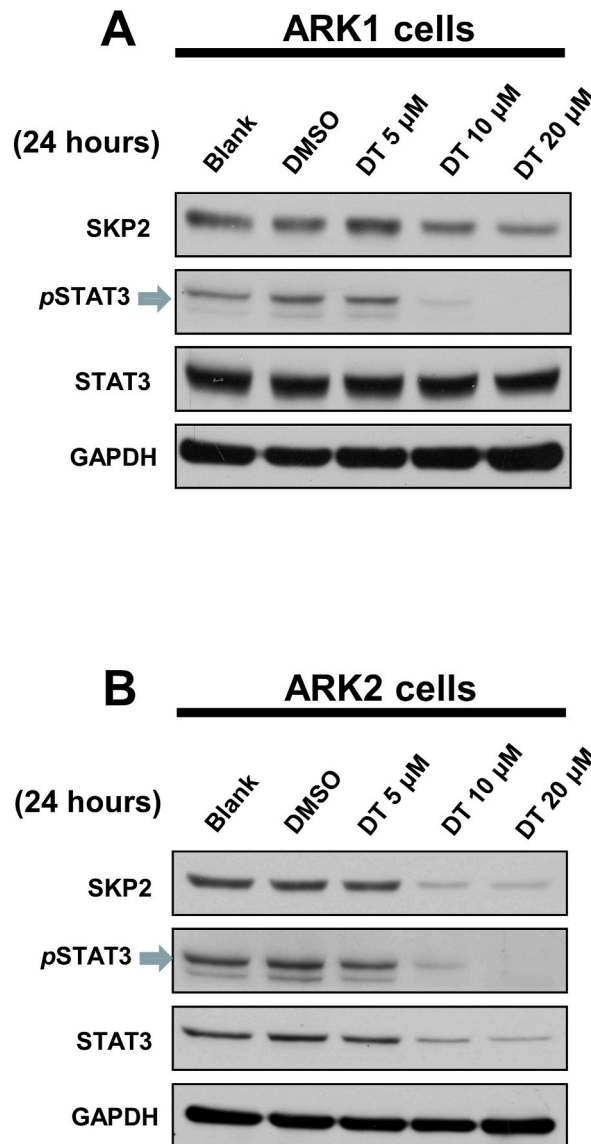
Fig. 4. Total cell extracts of ARK1 cells (A) or ARK2 cells (B) were harvested from cells treated with DMSO or indicated concentrations of DT for indicated hours. The protein was immunoblotted with polyclonal antibodies specific for SKP2, pSTAT3 and STAT3. GAPDH was used as an internal loading control.
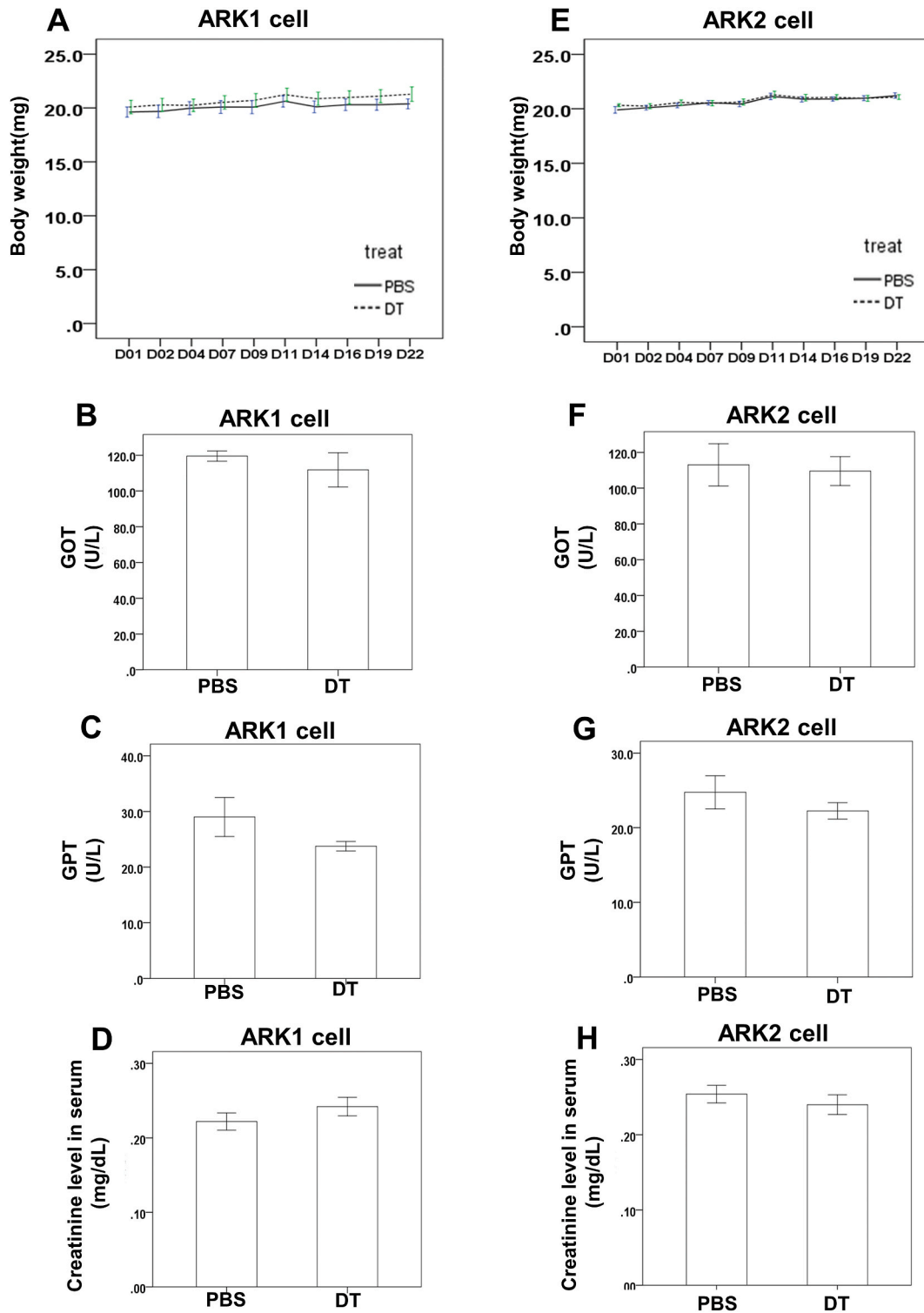
Fig. 5. The in vivo effect of DT on xenograft nude mice model. **A, E** Average mice weights with vehicle/DT (30 mg/kg via intraperitoneal injection, every 2 days) over a time course of 3 weeks in ARK1 cells (A) or ARK2 cells (E) xenograft nude mice model. **B, C, D, F, G, H** Creatinine (B, F), glutamic oxaloacetic transaminase (GOT) (C, G) and glutamic pyruvic transaminase (GPT) (D, H) levels in serum of mice after the treatment of vehicle or DT. All the results are representative of at least three independent experiments. (Error bars = mean ± S.E.M. Asterisks (*) mark samples significantly different from control group with p < 0.05).

preserving a reducing environment that reduces the levels of ROS and serves as a vital cellular antioxidant. Furthermore, the absence of GPX4, which converts GSH into GSSG, can result in a significant increase in GSSG, leading to a decline in the GSH/GSSG ratio. Additionally, GPX4 protects cells from ferroptosis by eliminating lipid ROS within the cell, and disrupting GPX4 function can trigger ferroptosis [7,8,19–23]. The inhibition of GPX4 expression by DT has been shown to induce apoptosis and ferroptosis in breast and lung cancer cells [11,16], raising the possibility that it could also induce ferroptosis in human endometrial cancer cells. To validate how DT affects endometrial cancer cells, we investigated its mode of action concerning ferroptosis. In our findings, it was observed that 10 μM DT led to a reduction in the GPX activity of ARK1 cells (Fig. 3A) and ARK2 cells (Fig. 3E) after 24 h. Additionally, the protein expression of GPX4 in ARK1 cells (Fig. 3B) and ARK2 cells (Fig. 3F) was significantly inhibited by 10 μM DT after 24 h. After 24 h, the levels of GSH were notably decreased in both ARK1 cells (Fig. 3C) and ARK2 cells (Fig. 3G) by 10 μM DT. Furthermore, the GSH/GSSG ratio in ARK1 cells (Fig. 3D) and ARK2 cells (Fig. 3H) was also decreased by 10 μM DT. These findings suggest that the inhibition of GPX4 expression caused by 10 μM DT triggered ferroptosis as a mechanism of cell death in endometrial cancer cells.
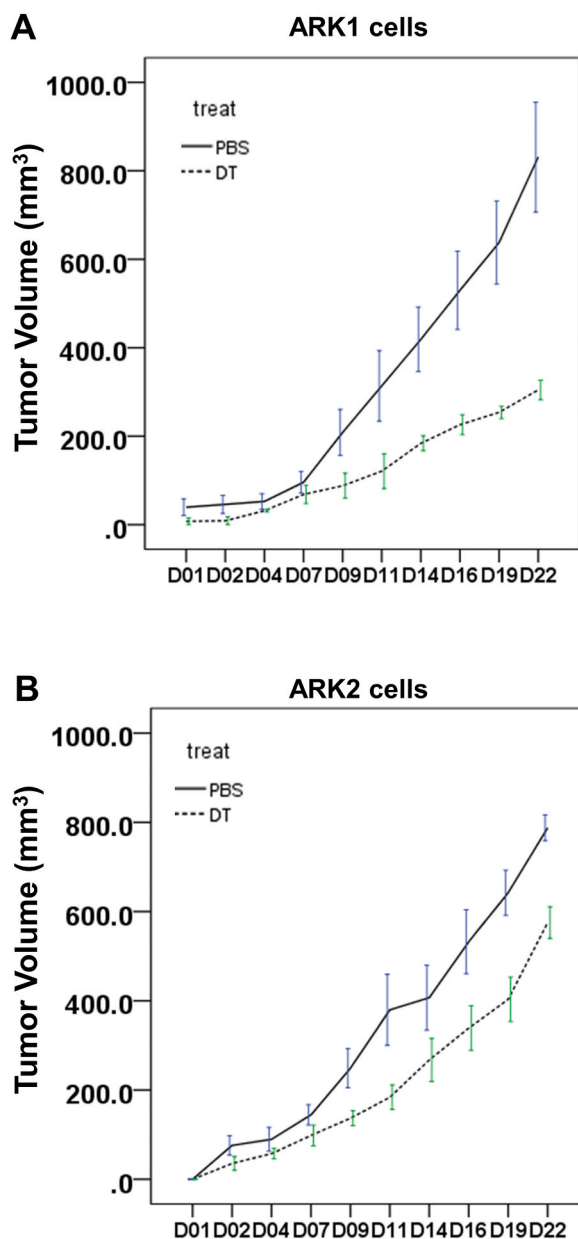
Fig. 6. The in vivo anti-tumor effect of DT on xenograft nude mice model. Average tumor volume of mice injected with either vehicle (DMSO) or DT (30 mg/kg via intraperitoneal injection, n = 5 per group) over a time course of 3 weeks in ARK1 cells (A) or ARK2 cells (E) xenograft nude mice model. (Error bars = mean ± S.E.M.).

3.4. Effects of DT on STAT3 phosphorylation, SKP2 protein expression of endometrial cancer cells

STAT3 (Signal transducer and activator of transcription 3) serves as a pivotal regulator in the metastatic behavior of tumors, including lung neoplasms [24,25]. Additionally, STAT3 functions as an instrumental biomarker for prognostic evaluation and represents a viable therapeutic target in various solid malignancies [26]. The STAT3 inhibitor BBI608 has been demonstrated to diminish the viability of patient-derived primary cells in endometrial carcinoma at clinically relevant concentrations [27]. An alternative investigation demonstrated that the activation of Src and STAT3 is mediated by integrin α6β4, leading to inhibition of ferroptosis [28, 29]. Subsequent analyses were conducted to assess the impact of DT on the phosphorylation of STAT3 at Tyr705 (p-STAT3) utilizing Western blot techniques. The results indicated that DT, at concentrations ranging from 10 to 20 μM, effectively attenuated STAT3 phosphorylation in both ARK1 and ARK2 cellular models (Fig. 4A). Additionally, a reduction in STAT3 protein levels was observed in ARK2 cells when treated with DT at the aforementioned concentrations (Fig. 4B).

SKP2 (S-phase kinase-associated protein 2), recognized as a downstream transcriptional effector of STAT3 [30], is pivotal in modulating both the metastatic and proliferative characteristics of neoplastic conditions [31–33]. Increased levels of SKP2 expression have been observed in endometrial malignancies and are correlated with unfavorable prognostic indicators [34]. Prior research has elucidated that YAP (Yes-associated protein 1) facilitates ferroptosis via the modulation of SKP2 expression [35]. Subsequent analyses were performed to assess the protein expression profiles of SKP2 in endometrial cancer cells treated with DT. Western blotting assays indicated a reduction in SKP2 protein levels in both ARK1 and ARK2 cell lines post-DT administration (Fig. 4A and B).

3.5. In vivo effect of DT on xenograft nude mouse model

In order to explore the impact of DT in vivo, we employed female mice with a tumor xenograft as a cancer model. Previous research indicated that treatment with DT (30 mg/kg via intraperitoneal injection) effectively suppressed the ultimate tumor volume in mice xenografted with either HCT-116 cells (colon cancer) or MCF-7 cells (breast cancer) [12,16]. Thus, we administered 30 mg/kg DT intraperitoneally to mice xenografted with either ARK1 or ARK2 cells. Following 3 weeks of DT treatment, we noted no instances of mouse mortality, and no noteworthy changes in either mouse activity or body weight were observed for ARK1 cell-xenografted mice (Fig. 5A) and ARK2 cell-xenografted mice (Fig. 5E). Additionally, levels of serum creatinine, glutamic oxaloacetic transaminase, and glutamic pyruvic transaminase remained unchanged between the DT group and control group (Fig. 5B, C, D, F, G, H), indicating that DT did not result in significant nephrotoxicity or hepatotoxicity in mice with ARK1 and ARK2 cell xenografts. Additionally, we observed that DT treatment resulted in a significant reduction in the ultimate tumor volume in both ARK1 cell-xenografted mice (Fig. 6A) and ARK2 cell-xenografted mice (Fig. 6B) after a 3-week period. These findings support our cell line data, indicating that DT treatment (30 mg/kg via intraperitoneal injection) effectively curbed the final tumor volume without any unfavorable effects in a xenograft nude mouse model.

4. Discussion

A recent investigation has established a strong connection between ferroptosis and drug resistance in endometrial cancer [36]. Earlier research has revealed that patients with a lower ferroptosis score are at a higher risk of developing resistance to cisplatin and paclitaxel, based on clinical samples of both tumor and normal tissues [37]. Furthermore, the activation of the HSPA5-GPX4 pathway, which induces ferroptosis resistance, can lead to gemcitabine resistance in ovarian cancer [38]. Therefore, targeting genes associated with ferroptosis could potentially be an effective treatment strategy for endometrial cancer [9]. The STAT3 inhibitor BBI608 has been demonstrated to diminish the viability of patient-derived primary cells in endometrial carcinoma at clinically relevant concentrations [27]. An alternative investigation demonstrated that the activation of Src and STAT3 is mediated by integrin α6β4, leading to inhibition of ferroptosis [28,29]. In our research, we observed that the viability of both ARK1 and ARK2 cells was significantly reduced by 10 μM DT. Additionally, DT at this concentration induced ferroptosis in endometrial cancer cells by inhibiting the expression of GPX4 and p-STAT3. Notably, the inhibitory effect of 10 μM DT was higher than that of commonly used clinical anti-cancer agents, such as oxaliplatin, gemcitabine, and 5-fluorouracil, in both ARK1 and ARK2 cells. These results suggest that 10 μM DT may have potential as an anti-tumor agent for endometrial cancer with drug resistance.

Kong et al. delineated the molecular architecture of Dihydroisotanshinone I [39]. Subsequent research has demonstrated the significant cardiovascular benefits of unrefined *Salvia miltiorrhiza Bunge* extracts, including coronary artery relaxation, myocardial antioxidant rescue, platelet aggregation inhibition, and the prevention of low-density lipoprotein oxidation. Additionally, these extracts have been shown to enhance the long-term memory retention in rodent models [40–42]. Furthermore, *Salvia miltiorrhiza* Bunge extracts have displayed anti-neoplastic properties across a range of human cancer cell types, such as gastric adenocarcinoma, prostate carcinoma, breast adenocarcinoma, colorectal carcinoma, and lung adenocarcinoma cells [43]. Notably, dihydrotanshinone I was found to possess elevated cytotoxic capabilities relative to other tanshinones in a majority of the evaluated cancer cell lines [43]. Separate investigations have also revealed that a purified form of *Salvia miltiorrhiza* Bunge extract, known as PF2401-SF, offers hepatoprotective effects in vivo and markedly attenuates inflammation in rat models of acute arthritis induced by carrageenan or dextran [44,45]. In a recent investigation, the administration of C-DM1 extract, which comprises constituents such as dihydroisotanshinone, dihydroisotanshinone I, cryptotanshinone, harpagoside, and atractyloside A, was found to ameliorate symptoms of diabetes in high-fat diet-induced diabetes mice [46]. Concurrently, another research endeavor demonstrated that dihydroisotanshinone I mitigates cellular apoptosis and exerts antioxidative properties by diminishing reactive oxygen species levels. Additionally, this compound modulates circadian gene expression, specifically by upregulating SIRT1 and downregulating BMAL1, in an in vitro

model of 6-OHDA-induced Parkinson's disease [47]. Separate investigations have also revealed that dihydroisotanshinone I triggers apoptosis in Detroit 562 cells, partially mediated through the p38 signaling pathway. Dihydroisotanshinone I was effective in shrinking head and neck squamous cell tumors without manifesting discernible hepatotoxic side effects in a xenograft murine model [48]. Studies conducted recently have revealed that various fat-soluble constituents found in *Salvia miltiorrhiza* (Danshen), such as tanshinone II, tanshinone I, cryptotanshinone, and DT, exhibit promising in vivo and in vitro antitumor effects against gynecological cancer, operating through distinct molecular mechanisms [49]. DT has been found to exhibit inhibitory effects against various forms of gynecological cancer, such as breast cancer, cervical cancer, and ovarian cancer, through several mechanisms [16,49–54]. In endometrial cancer, tanshinone I has been shown to impede the proliferation of HEC-1-A cells in a dose-dependent manner by inducing apoptosis and elevating the ROS level [55]. During our study, we noticed a significant decrease in cell viability for both ARK1 and ARK2 cells when exposed to a concentration of 10 μM DT. It is plausible that other tanshinone family members, including tanshinone I, tanshinone IIA, and cryptotanshinone, which possess similar chemical structures to DT, may also exhibit inhibitory effects against endometrial cancer. In previous study, the IC50 of tanshinone I against HEC-1-A cells was determined to be 20 μM following 24-h incubation [55]. In our study, we observed that DT exhibited an IC50 of 9.353 μM and 2.495 μM after being incubated for 24 h on ARK1 and ARK2 cells, respectively. It is worth noting that while HEC-1-A cells are endometrial adenocarcinoma, ARK1 and ARK2 cells are endometrial serous adenocarcinoma, which may account for the difference in IC50 between DT and tanshinone I. Another possible explanation is the difference in the side chains between DT and tanshinone I. Further research on the inhibitory effects of other members of the tanshinone family, including tanshinone II and cryptotanshinone, on endometrial cancer may be necessary.

In phytochemical derivatives, both juglone and plumbagin are naturally occurring quinones proven to instigate apoptotic pathways in endometrial cancer cells [56,57]. Juglone further elicits ferroptosis in Ishikawa cells of endometrial cancer origin by facilitating intracellular iron sequestration and glutathione (GSH) depletion [58]. Previous research has elucidated that tanshinone IIA provokes ferroptosis in gastric carcinoma cell lines BGC-823 and NCI–H87 through the upregulation of p53 and the downregulation of xCT (SLC7A11) [59]. Tanshinone IIA also attenuates the stem cell-like properties of gastric cancer cells by inducing ferroptosis, accompanied by an increase in lipid peroxide concentrations and a decrease in glutathione levels [60]. Our investigations have confirmed that DT induces ferroptosis across multiple cancer types, including endometrial, breast, and lung cancers, via the suppression of GPX4 expression [11,16]. Structurally analogous compounds within the tanshinone family may similarly hold the capacity to inhibit GPX4 and thereby initiate ferroptosis. Separate studies have revealed that integrin α6β4-mediated activation of Src and STAT3 serves as a mechanism for ferroptosis inhibition [28,29]. YAP facilitates ferroptosis via the modulation of SKP2 expression [35]. In our experiments, we noted a marked reduction in cell viability for both ARK1 and ARK2 cells when exposed to 10 μM DT. Concurrently, this concentration of DT suppressed the expression of GPX4, phosphorylated STAT3 and SKP2, thereby inducing ferroptosis in endometrial cancer cells. The possibility remains that DT could activate ferroptosis pathways independent of GPX4 inhibition.

In the current investigation, limitations arise from the utilization of only two types of endometrial cancer cells, namely ARK1 and ARK2. A more comprehensive understanding could be achieved by incorporating additional endometrial cancer cell types such as Ishikawa, HEC-1-A, HEC-1-B, and KLE cells, each possessing distinct cellular characteristics. This would facilitate a more robust validation of DT's effects on endometrial cancer prior to clinical trials [61]. Furthermore, the structural similarities among various members of the tanshinones family with DT warrant exploration in future research to identify more efficacious compounds. Regarding in vivo studies, the xenografted animal model employed involved ARK1 and ARK2 cells, both of human origin. To enhance the translational relevance, alternative animal models such as spontaneous or chemically induced endometrial cancer rodent models, as well as transgenic mouse models, should be considered for future investigations before proceeding to clinical trials [62].

5. Conclusion

To summarize, our findings indicate that a concentration of 10 μM DT can impede the cell viability of endometrial cancer cells via apoptosis and ferroptosis. The mechanism by which 10 μM DT elicits ferroptosis is through the inhibition of GPX4 expression. Additionally, in a xenograft nude mice model, DT treatment (30 mg/kg via intraperitoneal injection) effectively decreased the final tumor volume without any detrimental effects. Therefore, DT may serve as a promising therapeutic option for the treatment of endometrial cancer. Further research is warranted to verify these results.

Chemical compounds studied in this article

Dihydroisotanshinone I (PubChem CID:89406)

Availability of data and materials

All data generated or analyzed during this study are indicated in this article (with no patient data). The datasets generated during and/or analyzed during the current study are available from the corresponding author on reasonable request.

Ethics approval and consent to participate

Studies involving animals were approved by Animal Care and Use Committee (Approval number: 2020032305) of Chang Gung Memory Hospital.

Consent for publication

Not applicable (not contain any individual person's data).

Declaration of competing interest

The authors declare the following financial interests/personal relationships which may be considered as potential competing interests:

Ching-Yuan Wu reports financial support was provided by Chiayi Chang Gung Memorial Hospital. Ching-Yuan Wu reports a relationship with Chiayi Chang Gung Memorial Hospital that includes: funding grants.

Acknowledgements

The authors acknowledge the Health Information and Epidemiology Laboratory at the Chiayi Chang Gung Memorial Hospital for the comments and assistance in data analysis and kindly gifts from Dr. Tzu-Hao Wang (Department of Obstetrics and Gynecology, Chang Gung Memorial Hospital and Chang Gung University).

Appendix A. Supplementary data

Supplementary data to this article can be found online at https://doi.org/10.1016/j.heliyon.2023.e21652.

Abbreviations

GPX4	Glutathione peroxidase 4
DT	dihydroisotanshinone I
GSH	reduced glutathione
STAT3	Signal transducer and activator of transcription 3
SKP2	S-phase kinase-associated protein 2

References

[1] R.L. Siegel, K.D. Miller, A. Jemal, Cancer statistics, 2018, CA Cancer J Clin 68 (1) (2018) 7–30.
[2] R.E. Bristow, M.J. Zerbe, N.B. Rosenshein, F.C. Grumbine, F.J. Montz, Stage IVB endometrial carcinoma: the role of cytoreductive surgery and determinants of survival, Gynecol. Oncol. 78 (2) (2000) 85–91.
[3] J. McEachron, C. Chatterton, V. Hastings, C. Gorelick, K. Economos, Y.C. Lee, M.J. Kanis, A clinicopathologic study of endometrial cancer metastatic to bone: identification of microsatellite instability improves treatment strategies, Gynecol Oncol Rep 32 (2020), 100549.
[4] M.J. Carlson, K.W. Thiel, K.K. Leslie, Past, present, and future of hormonal therapy in recurrent endometrial cancer, Int J Womens Health 6 (2014) 429–435.
[5] N. Kajarabille, G.O. Latunde-Dada, Programmed cell-death by ferroptosis: antioxidants as mitigators, Int. J. Mol. Sci. 20 (19) (2019).
[6] G.C. Forcina, S.J. Dixon, GPX4 at the crossroads of lipid homeostasis and ferroptosis, Proteomics 19 (18) (2019), e1800311.
[7] W.S. Yang, B.R. Stockwell, Ferroptosis: death by lipid peroxidation, Trends Cell Biol. 26 (3) (2016) 165–176.
[8] W.S. Yang, R. SriRamaratnam, M.E. Welsch, K. Shimada, R. Skouta, V.S. Viswanathan, J.H. Cheah, P.A. Clemons, A.F. Shamji, C.B. Clish, L.M. Brown, A. W. Girotti, V.W. Cornish, S.L. Schreiber, B.R. Stockwell, Regulation of ferroptotic cancer cell death by GPX4, Cell 156 (1–2) (2014) 317–331.
[9] J. Wu, L. Zhang, S. Wu, Z. Liu, Ferroptosis: opportunities and challenges in treating endometrial cancer, Front. Mol. Biosci. 9 (2022), 929832.
[10] A. Lopez-Janeiro, I. Ruz-Caracuel, J.L. Ramon-Patino, V. De Los Rios, M. Villalba Esparza, A. Berjon, L. Yebenes, A. Hernandez, I. Masetto, E. Kadioglu, V. Goubert, V. Heredia-Soto, R. Barderas, J.I. Casal, C.E. de Andrea, A. Redondo, M. Mendiola, A. Pelaez-Garcia, D. Hardisson, Proteomic analysis of low-grade, early-stage endometrial carcinoma reveals new dysregulated pathways associated with cell death and cell signaling, Cancers 13 (4) (2021).
[11] C.Y. Wu, Y.H. Yang, Y.S. Lin, G.H. Chang, M.S. Tsai, C.M. Hsu, R.A. Yeh, L.H. Shu, Y.C. Cheng, H.T. Liu, Dihydroisotanshinone I induced ferroptosis and apoptosis of lung cancer cells, Biomed. Pharmacother. 139 (2021), 111585.
[12] Y.Y. Lin, I.Y. Lee, W.S. Huang, Y.S. Lin, F.C. Kuan, L.H. Shu, Y.C. Cheng, Y.H. Yang, C.Y. Wu, Danshen improves survival of patients with colon cancer and dihydroisotanshinone I inhibit the proliferation of colon cancer cells via apoptosis and skp2 signaling pathway, J. Ethnopharmacol. 209 (2017) 305–316.
[13] M. Baysal, S. Ilgin, G. Kilic, V. Kilic, S. Ucarcan, O. Atli, Reproductive toxicity after levetiracetam administration in male rats: evidence for role of hormonal status and oxidative stress, PLoS One 12 (4) (2017), e0175990.
[14] O.J. Onaolapo, M.A. Adekola, T.O. Azeez, K. Salami, A.Y. Onaolapo, l-Methionine, silymarin, A comparison of prophylactic protective capabilities in acetaminophen-induced injuries of the liver, kidney and cerebral cortex, Biomedicine & pharmacotherapy = Biomedecine & pharmacotherapie 85 (2017) 323–333.
[15] C.Y. Wu, J.Y. Cherng, Y.H. Yang, C.L. Lin, F.C. Kuan, Y.Y. Lin, Y.S. Lin, L.H. Shu, Y.C. Cheng, H.T. Liu, M.C. Lu, J. Lung, P.C. Chen, H.K. Lin, K.D. Lee, Y.H. Tsai, Danshen improves survival of patients with advanced lung cancer and targeting the relationship between macrophages and lung cancer cells, Oncotarget 8 (53) (2017) 90925–90947.

[16] Y.S. Lin, Y.C. Shen, C.Y. Wu, Y.Y. Tsai, Y.H. Yang, Y.Y. Lin, F.C. Kuan, C.N. Lu, G.H. Chang, M.S. Tsai, C.M. Hsu, R.A. Yeh, P.R. Yang, I.Y. Lee, L.H. Shu, Y. C. Cheng, H.T. Liu, Y.H. Wu, Y.H. Wu, D.C. Chang, Danshen improves survival of patients with breast cancer and dihydroisotanshinone I induces ferroptosis and apoptosis of breast cancer cells, Front. Pharmacol. 10 (2019) 1226.

[17] C.Y. Wu, Y.H. Yang, Y.Y. Lin, F.C. Kuan, Y.S. Lin, W.Y. Lin, M.Y. Tsai, J.J. Yang, Y.C. Cheng, L.H. Shu, M.C. Lu, Y.J. Chen, K.D. Lee, H.Y. Kang, Anti-cancer effect of danshen and dihydroisotanshinone I on prostate cancer: targeting the crosstalk between macrophages and cancer cells via inhibition of the STAT3/CCL2 signaling pathway, Oncotarget 8 (25) (2017) 40246–40263.

[18] X. Chen, P.B. Comish, D. Tang, R. Kang, Characteristics and biomarkers of ferroptosis, Front. Cell Dev. Biol. 9 (2021), 637162.

[19] T.M. Seibt, B. Proneth, M. Conrad, Role of GPX4 in ferroptosis and its pharmacological implication, Free Radic. Biol. Med. 133 (2019) 144–152.

[20] O. Canli, Y.B. Alankus, S. Grootjans, N. Vegi, L. Hultner, P.S. Hoppe, T. Schroeder, P. Vandenabeele, G.W. Bornkamm, F.R. Greten, Glutathione peroxidase 4 prevents necroptosis in mouse erythroid precursors, Blood 127 (1) (2016) 139–148.

[21] P. Lei, T. Bai, Y. Sun, Mechanisms of ferroptosis and relations with regulated cell death: a review, Front. Physiol. 10 (2019) 139.

[22] Y. Kinowaki, M. Kurata, S. Ishibashi, M. Ikeda, A. Tatsuzawa, M. Yamamoto, O. Miura, M. Kitagawa, K. Yamamoto, Glutathione peroxidase 4 overexpression inhibits ROS-induced cell death in diffuse large B-cell lymphoma, Lab. Invest. 98 (5) (2018) 609–619.

[23] J. Li, F. Cao, H.L. Yin, Z.J. Huang, Z.T. Lin, N. Mao, B. Sun, G. Wang, Ferroptosis: past, present and future, Cell Death Dis. 11 (2) (2020) 88.

[24] E. Bonastre, S. Verdura, I. Zondervan, F. Facchinetti, S. Lantuejoul, M.D. Chiara, J.P. Rodrigo, J. Carretero, E. Condom, A. Vidal, D. Sidransky, A. Villanueva, L. Roz, E. Brambilla, S. Savola, M. Sanchez-Cespedes, PARD3 inactivation in lung squamous cell carcinomas impairs STAT3 and promotes malignant invasion, Cancer Res. 75 (7) (2015) 1287–1297.

[25] E. Devarajan, S. Huang, STAT3 as a central regulator of tumor metastases, Curr. Mol. Med. 9 (5) (2009) 626–633.

[26] P. Wu, D. Wu, L. Zhao, L. Huang, G. Shen, Y. Chai, Prognostic Role of STAT3 in Solid Tumors: a Systematic Review and Meta-Analysis, Oncotarget, 2016.

[27] J. Chen, S. Huang, H. Li, Y. Li, H. Zeng, J. Hu, Y. Lin, H. Cai, P. Deng, T. Song, T. Guan, H. Zeng, M. Liu, STAT3 inhibitor BBI608 reduces patient-specific primary cell viability of cervical and endometrial cancer at a clinical-relevant concentration, Clin. Transl. Oncol. 25 (3) (2023) 662–672.

[28] H.F. Yan, T. Zou, Q.Z. Tuo, S. Xu, H. Li, A.A. Belaidi, P. Lei, Ferroptosis: mechanisms and links with diseases, Signal Transduct Target Ther 6 (1) (2021) 49.

[29] C.W. Brown, J.J. Amante, H.L. Goel, A.M. Mercurio, The alpha6beta4 integrin promotes resistance to ferroptosis, J. Cell Biol. 216 (12) (2017) 4287–4297.

[30] H. Huang, W. Zhao, D. Yang, Stat3 induces oncogenic Skp2 expression in human cervical carcinoma cells, Biochem. Biophys. Res. Commun. 418 (1) (2012) 186–190.

[31] C.Q. Zhu, F.H. Blackhall, M. Pintilie, P. Iyengar, N. Liu, J. Ho, T. Chomiak, D. Lau, T. Winton, F.A. Shepherd, M.S. Tsao, Skp2 gene copy number aberrations are common in non-small cell lung carcinoma, and its overexpression in tumors with ras mutation is a poor prognostic marker, Clin. Cancer Res. : an official journal of the American Association for Cancer Research 10 (6) (2004) 1984–1991.

[32] A. Osoegawa, I. Yoshino, S. Tanaka, K. Sugio, T. Kameyama, M. Yamaguchi, Y. Maehara, Regulation of p27 by S-phase kinase-associated protein 2 is associated with aggressiveness in non-small-cell lung cancer, J. Clin. Oncol. : official journal of the American Society of Clinical Oncology 22 (20) (2004) 4165–4173.

[33] A. Feizi, S. Bordel, Metabolic and protein interaction sub-networks controlling the proliferation rate of cancer cells and their impact on patient survival, Sci. Rep. 3 (2013) 3041.

[34] D. Frescas, M. Pagano, Deregulated proteolysis by the F-box proteins SKP2 and beta-TrCP: tipping the scales of cancer, Nat. Rev. Cancer 8 (6) (2008) 438–449.

[35] W.H. Yang, C.C. Lin, J. Wu, P.Y. Chao, K. Chen, P.H. Chen, J.T. Chi, The hippo pathway effector YAP promotes ferroptosis via the E3 ligase SKP2, Mol. Cancer Res. 19 (6) (2021) 1005–1014.

[36] J. He, H. Ding, H. Li, Z. Pan, Q. Chen, Intra-tumoral expression of SLC7A11 is associated with immune microenvironment, drug resistance, and prognosis in cancers: a pan-cancer analysis, Front. Genet. 12 (2021), 770857.

[37] H. Wang, Y. Wu, S. Chen, M. Hou, Y. Yang, M. Xie, Construction and validation of a ferroptosis-related prognostic model for endometrial cancer, Front. Genet. 12 (2021), 729046.

[38] S. Zhu, Q. Zhang, X. Sun, H.J. Zeh 3rd, M.T. Lotze, R. Kang, D. Tang, HSPA5 regulates ferroptotic cell death in cancer cells, Cancer Res. 77 (8) (2017) 2064–2077.

[39] D.Y. Kong, X.J. Liu, [Structure of dihydroisotanshinone I of danshen], Yao Xue Xue Bao 19 (10) (1984) 755–759.

[40] B.-Q. Wang, Salvia miltiorrhiza: chemical and pharmacological review of a medicinal plant, J. Med. Plants Res. 4 (25) (2010) 2813–2820.

[41] J.Y. Han, J.Y. Fan, Y. Horie, S. Miura, D.H. Cui, H. Ishii, T. Hibi, H. Tsuneki, I. Kimura, Ameliorating effects of compounds derived from Salvia miltiorrhiza root extract on microcirculatory disturbance and target organ injury by ischemia and reperfusion, Pharmacol. Ther. 117 (2) (2008) 280–295.

[42] T.H. Lin, C.L. Hsieh, Pharmacological effects of Salvia miltiorrhiza (Danshen) on cerebral infarction, Chin. Med. 5 (2010) 22.

[43] B. Sung, H.S. Chung, M. Kim, Y.J. Kang, D.H. Kim, S.Y. Hwang, M.J. Kim, C.M. Kim, H.Y. Chung, N.D. Kim, Cytotoxic effects of solvent-extracted active components of Salvia miltiorrhiza Bunge on human cancer cell lines, Exp. Ther. Med. 9 (4) (2015) 1421–1428.

[44] W.Y. Jiang, B.H. Jeon, Y.C. Kim, S.H. Lee, D.H. Sohn, G.S. Seo, PF2401-SF, standardized fraction of Salvia miltiorrhiza shows anti-inflammatory activity in macrophages and acute arthritis in vivo, Int Immunopharmacol 16 (2) (2013) 160–164.

[45] E.J. Park, Y.Z. Zhao, Y.C. Kim, D.H. Sohn, Preventive effects of a purified extract isolated from Salvia miltiorrhiza enriched with tanshinone I, tanshinone IIA and cryptotanshinone on hepatocyte injury in vitro and in vivo, Food Chem. Toxicol. 47 (11) (2009) 2742–2748.

[46] P. Wang, Y. Liu, S.Y. Kang, C. Lyu, X. Han, T. Ho, K.J. Lee, X. Meng, Y.K. Park, H.W. Jung, Clean-DM1, a Korean polyherbal formula, improves high fat diet-induced diabetic symptoms in mice by regulating IRS/PI3K/AKT and AMPK expressions in pancreas and liver tissues, Chin. J. Integr. Med. (2023), https://doi.org/10.1007/s11655-023-3548-9.

[47] H.C. Su, Y.T. Sun, M.Y. Yang, C.Y. Wu, C.M. Hsu, Dihydroisotanshinone I and BMAL-SIRT1 pathway in an in vitro 6-OHDA-induced model of Parkinson's disease, Int. J. Mol. Sci. 24 (13) (2023).

[48] C.M. Hsu, M.Y. Yang, M.S. Tsai, G.H. Chang, Y.H. Yang, Y.T. Tsai, C.Y. Wu, S.F. Chang, Dihydroisotanshinone I as a treatment option for head and neck squamous cell carcinomas, Int. J. Mol. Sci. 22 (16) (2021).

[49] Z. Jin, Y. Chenghao, P. Cheng, Anticancer effect of tanshinones on female breast cancer and gynecological cancer, Front. Pharmacol. 12 (2021), 824531.

[50] Y. Ye, W. Xu, W. Zhong, Y. Li, C. Wang, Combination treatment with dihydrotanshinone I and irradiation enhances apoptotic effects in human cervical cancer by HPV E6 down-regulation and caspases activation, Mol. Cell. Biochem. 363 (1–2) (2012) 191–202.

[51] H. Zhao, Y. Liang, C. Sun, Y. Zhai, X. Li, M. Jiang, R. Yang, X. Li, Q. Shu, G. Kai, B. Han, Dihydrotanshinone I inhibits the lung metastasis of breast cancer by suppressing neutrophil extracellular traps formation, Int. J. Mol. Sci. 23 (23) (2022).

[52] A. Kashyap, S.M. Umar, J.R.A. Dev, C.P. Prasad, Dihydrotanshinone-I modulates epithelial mesenchymal transition (EMT) thereby impairing migration and clonogenicity of triple negative breast cancer cells, Asian Pac J Cancer Prev 22 (7) (2021) 2177–2184.

[53] S.L. Tsai, F.M. Suk, C.I. Wang, D.Z. Liu, W.C. Hou, P.J. Lin, L.F. Hung, Y.C. Liang, Anti-tumor potential of 15,16-dihydrotanshinone I against breast adenocarcinoma through inducing G1 arrest and apoptosis, Biochem. Pharmacol. 74 (11) (2007) 1575–1586.

[54] X. Wang, X. Xu, G. Jiang, C. Zhang, L. Liu, J. Kang, J. Wang, L. Owusu, L. Zhou, L. Zhang, W. Li, Dihydrotanshinone I inhibits ovarian cancer cell proliferation and migration by transcriptional repression of PIK3CA gene, J. Cell Mol. Med. 24 (19) (2020) 11177–11187.

[55] Q. Li, J. Zhang, Y. Liang, W. Mu, X. Hou, X. Ma, Q. Cao, Tanshinone l exhibits anticancer effects in human endometrial carcinoma HEC-1-A cells via mitochondrial mediated apoptosis, cell cycle arrest and inhibition of JAK/STAT signalling pathway, J BUON 23 (4) (2018) 1092–1096.

[56] Y.Y. Zhang, F. Zhang, Y.S. Zhang, K. Thakur, J.G. Zhang, Y. Liu, H. Kan, Z.J. Wei, Mechanism of juglone-induced cell cycle arrest and apoptosis in Ishikawa human endometrial cancer cells, J. Agric. Food Chem. 67 (26) (2019) 7378–7389.

[57] X. Zhang, H. Kan, Y. Liu, W. Ding, Plumbagin induces Ishikawa cell cycle arrest, autophagy, and apoptosis via the PI3K/Akt signaling pathway in endometrial cancer, Food Chem. Toxicol. 148 (2021), 111957.

[58] Y.Y. Zhang, Z.J. Ni, E. Elam, F. Zhang, K. Thakur, S. Wang, J.G. Zhang, Z.J. Wei, Juglone, a novel activator of ferroptosis, induces cell death in endometrial carcinoma Ishikawa cells, Food Funct. 12 (11) (2021) 4947–4959.

[59] Z. Guan, J. Chen, X. Li, N. Dong, Tanshinone IIA induces ferroptosis in gastric cancer cells through p53-mediated SLC7A11 down-regulation, Biosci. Rep. 40 (8) (2020).

[60] H. Ni, G. Ruan, C. Sun, X. Yang, Z. Miao, J. Li, Y. Chen, H. Qin, Y. Liu, L. Zheng, Y. Xing, T. Xi, X. Li, Tanshinone IIA inhibits gastric cancer cell stemness through inducing ferroptosis, Environ. Toxicol. 37 (2) (2022) 192–200.

[61] J. Kozak, P. Wdowiak, R. Maciejewski, A. Torres, A guide for endometrial cancer cell lines functional assays using the measurements of electronic impedance, Cytotechnology 70 (1) (2018) 339–350.

[62] T. Van Nyen, C.P. Moiola, E. Colas, D. Annibali, F. Amant, Modeling endometrial cancer: past, present, and future, Int. J. Mol. Sci. 19 (8) (2018).